

Two Novel Experimental Schemes for Terahertz Tomography

Till Mohr and Wolfgang Elsaßer*

Institute of Applied Physics, Technische Universität Darmstadt, Germany

* e-mail: Elsaesser@physik.tu-darmstadt.de

ABSTRACT

In this contribution, we present two novel and compact terahertz tomography spectroscopy concepts. First, we exploit continuous-wave (CW) terahertz radiation generation and phase-sensitive detection in the same single photoconductive antenna (PCA), a homodyne self-mixing detection approach and apply it within a 2D terahertz tomography imaging application where we reconstruct the two-dimensional image of a hollow-core Teflon cylinder filled with α -lactose as a proof-of-concept demonstration.

Second, we realize a single-pixel tomography scheme where 2D tomographic spatial information is achieved by spatially-resolved photodoping of a high-resistivity silicon wafer plate giving rise to fast transverse single-pixel information (via a digital micro mirror device (DMD)) with the subsequent rotation of the object for tomography. Both concepts offer a significantly reduced complexity and consequently lower cost of the terahertz spectroscopy set-up and their THz performance will be discussed and compared.

Keywords: terahertz radiation, terahertz imaging, tomographic imaging, single-pixel detection.

1. INTRODUCTION

Terahertz research is actually a booming field, with respect to both, a multitude of applications for terahertz radiation and also accompanied by new developments [1], as e.g. for spectroscopy and imaging. Terahertz imaging benefits from the opacity of many materials and the specific spectral finger-prints of a multitude of molecules located in the terahertz region. Here the spectrum of available implementations include optical [2], electro-optical [3] and electronic [4] schemes for the generation and detection of the terahertz radiation. Also the imaging techniques range from mechanically raster scanning systems [4] to multi-pixel detector arrays achieving large numbers of pixels [5] and high frame rates of up to 450 frames per second [6]. Another promising method is the ‘single pixel’ imaging, which uses a bucket detector and does not require any mechanically raster scanning of the object. This method reconstructs an image of the object by a set of measurements of the total intensity transmitted, reflected or scattered from the object under illumination of different spatially patterned radiation. Both, random [3] and Hadamard [7] based patterns, have successfully been used to perform imaging in the terahertz frequency range. Further promising progress of this method has been achieved in near field terahertz imaging, leading to sub-wavelength spatial resolution [8].

In this contribution, we show two novel and compact terahertz tomography spectroscopy concepts. The first concept utilizes the homodyne self-mixing (HSM) method [9], which combines generation and phase-sensitive detection of CW terahertz radiation in a single PCA (Section 2). Second, we realize a single-pixel tomography scheme where 2D tomographic spatial information is achieved by spatially-resolved photodoping of a high-resistivity silicon wafer plate (Section 3). In this scheme a broadband Hg-Arc lamp serves as a source of the terahertz radiation and a liquid He cooled bolometer is used as bucket detector. Both concepts are applied within a 2D terahertz tomography imaging application, where we reconstruct the two-dimensional image of different sample objects composed of diverse materials.

2. HOMODYNE SELF-MIXING

Opto-electronic photomixing is one of the most promising techniques for the generation and detection of pulsed THz radiation, with its application in time domain spectroscopy, or CW THz radiation, utilizing its narrow linewidth for finger print spectroscopy. This technique convinces by its robustness, compactness, phase sensitivity and good signal to noise ratio, which makes it a perfect option for many scientific and industrial tasks. Nevertheless, the development of novel concepts for generation and detection of THz radiation is an ongoing process. Promising progress is achieved by the combination of THz source and detector into one device, as the transfer of the self-mixing technique from near infrared laser diodes to THz quantum cascade lasers [2]. Here, we demonstrate a new approach which combines the generation and phase sensitive detection of CW THz radiation utilizing only one PCA, which leads to a simplification and cost reduction of the THz setup.

2.1 Experimental set-up

As in a conventional CW heterodyne set-up, the output of two single-mode semiconductor lasers at frequency ν_1 and ν_2 are superimposed to generate an optical beat signal at a difference frequency of $\nu_{\text{THz}} = (\nu_2 - \nu_1)$. As schematically depicted in Fig. 1, the lasers are two tunable external-cavity diode lasers (ECDLs) with a band-pass filter as frequency selective element, emitting at wavelengths of around 794 nm and providing an optical

output power of approximately 80 mW each. After coupling each laser beam into a single-mode fiber, they are superimposed via a fiber-based 50:50 beam combiner.

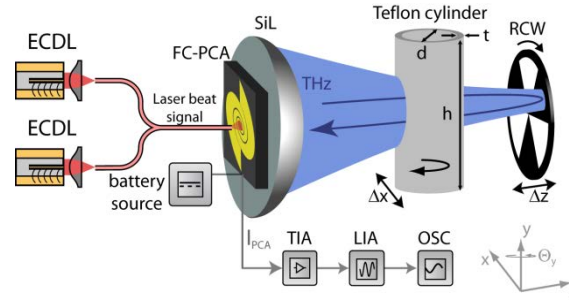


Figure 1. Schematic of the experimental set-up: ECDL external cavity diode laser; FC-PCA fiber coupled photoconductive antenna; SiL silicon lens; RCW revolving chopper wheel; TIA transimpedance amplifier; LIA lock-in amplifier OSC - digital oscilloscope.

The superimposed radiation of the two lasers impinges on a fiber-coupled PCA (FC-PCA: GaAs-based photomixer, model EK-000831, TOPTICA Photonics). The FC-PCA emits the terahertz radiation at the difference frequency of the two laser frequencies and a hyperhemispherical silicon lens (SiL), with a focal length of 40mm focuses the terahertz beam behind the PCA, resulting in a focus diameter of around 5 mm. The PCA is electrically connected to a 9V battery that provides a constant bias voltage. Within the Rayleigh length of the terahertz radiation a revolving chopper wheel is placed, which back reflects the terahertz radiation onto the FC-PCA. The chopper wheel revolves at a speed of up to 2.6 kHz and is mounted on a linear translation stage, allowing a variation of the phase between the laser beat signal and the back reflected THz radiation. The back-reflected terahertz radiation gives rise to the HSM intensity signal $I(z)$ [9], which is proportional to

$$I(z) = I_0 \cdot \cos\left(\frac{4\pi}{\lambda} \cdot z\right).$$

Here λ is the wavelength of the terahertz field and z the displacement of the RCW. In order to perform two-dimensional tomographic terahertz imaging a hollow-core Teflon cylinder filled with α -Lactose monohydrate powder is placed in between the FC-PCA and the RCW. The dimensions of the cylinder are height $h = 20$ mm, cylinder diameter $d = 18.5$ mm and wall-thickness $t = 4.25$ mm. This sample is mounted on a second linear translation stage allowing for a movement orthogonal to the terahertz beam (x direction) related to the RCW. A further rotation around the center axes of the Teflon cylinder is realized by a rotation platform. In this manner the sample is scanned over a range of 27 mm in 1mm steps in x -direction and for 6 rotation angles Θ_y between 0° and 150° in 30° iterations.

2.2 Experimental results and discussion

A normalized example of the measured HSM signals for $\Theta_y = 0^\circ$ at each x -position is shown in Fig. 2 for the two selected terahertz frequencies of 0.19 THz (left) and 0.539 THz (right). As a guide to the eye a photograph of half of the investigated Teflon cylinder is scaled to the axis dimensions and shown in the background in both graphs. The filled circles in blue represent a scan of the Teflon cylinder filled with α -Lactose monohydrate powder, whereas the empty circles in red show a scan of the empty hollow-core Teflon cylinder. The hollow-core Teflon cylinder filled with powder clearly shows negligible transmission through the whole sample at a terahertz frequency of 0.539 THz (Fig. 2 right, blue circles). Only in the periphery outside the Teflon cylinder, from $x = 0$ to $x = 4$ mm and from $x = 22$ to $x = 26$ mm, a considerable transmission is observed. In contrast for the empty cylinder at a terahertz frequency of 0.539 THz (Fig. 2 right, red empty circles) and for the filled cylinder for a terahertz frequency of 0.19 THz (Fig. 2 left, blue filled circles) a high transmission through the center of the sample can be seen, whereas no transmission through the side walls of the Teflon cylinder ($x=6$ to $x = 10$ mm and $x = 15$ to $x = 20$ mm) is observed in both cases. Responsible for the absence of any signal in case of the filled cylinder at 0.539 THz is not the scattering by the powder, but rather the characteristic absorption line of α -Lactose near the selected frequency of 0.539 THz [10].

The reconstructed two-dimensional images of the Teflon cylinder filled with α -Lactose monohydrate powder for both investigated terahertz frequencies of 0.19 THz (left) and 0.539 THz (right) are depicted in Fig. 3. In case of a terahertz frequency of 0.19 THz a transmission through the surrounding air can be seen at the edges of Teflon cylinder by the yellow and orange region. The side-walls of the Teflon cylinder are defined by a blue area of no transmittance, due to strong refraction on the curved surface of the Teflon cylinder. The center of the reconstructed image at 0.19 THz clearly shows a high transmission despite the α -Lactose inside the Teflon cylinder, which confirms our assumption that the scattering at the terahertz wavelength does not affect our transmission experiment. The right hand side of Fig. 3 shows a large blue region of no transmission, from which

the outer shape of the Teflon cylinder is recognized. Here, only a transmission through the air surrounding the cylinder can be seen.

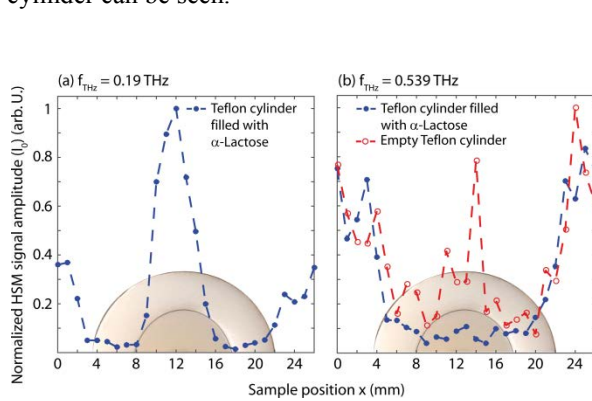


Figure 2. Obtained 1D projections for a sample scan in x -direction for a rotation angle Θ_y of 0° without (empty red circles) and with (filled blue circles) α -Lactose filling for terahertz frequencies of 0.19 THz (left) and 0.539 THz (right). A photograph of half of the investigated Teflon cylinder scaled to the axis dimensions should serve as a guide to the eye.

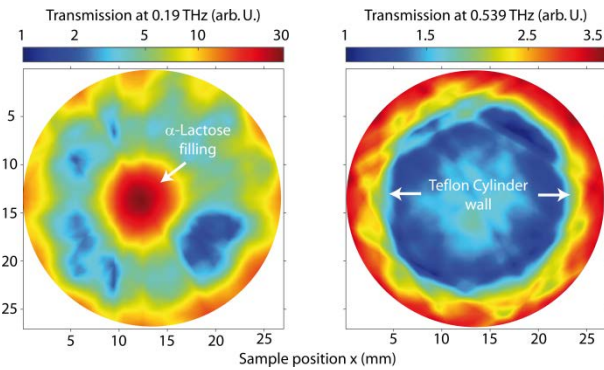


Figure 3. Reconstructed two-dimensional image in a logarithmic representation at a terahertz frequency of 0.19 THz (left) and 0.539 THz (right) of the Teflon cylinder filled with α -Lactose.

3. SINGLE PIXEL TOMOGRAPHIC IMAGING

By comparing tomographic imaging in the x-ray region to tomographic imaging in the terahertz spectral region several still remaining challenges for the terahertz region are noticed. First, the number of detectors providing spatial resolution with high signal to noise ratios is still limited. Second, optical effects like diffraction, reflection and refraction have a huge influence on the measured projections [11] as has been seen in the previous section (e.g. Fig. 2). To overcome the need of spatially resolving detectors and in order to reduce the influence of optical effects, single-pixel imaging could be a superior approach. This approach uses a large bucket detector, which measures the total intensity transmitted, reflected or scattered from an object under illumination of different spatially distributed light patterns. One possible choice as a set of patterns is the Hadamard matrix, whose rows are mutually orthogonal and represent one illumination pattern each.

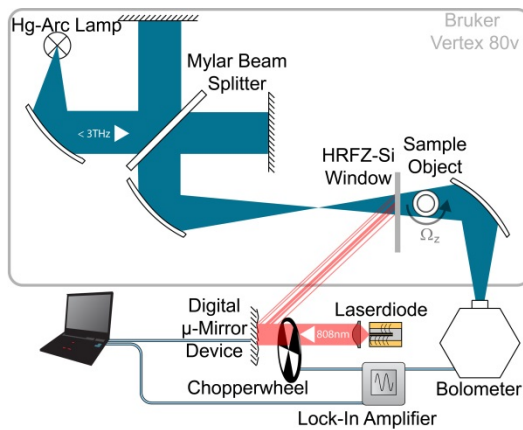


Figure 4. Schematic of the experimental set-up.

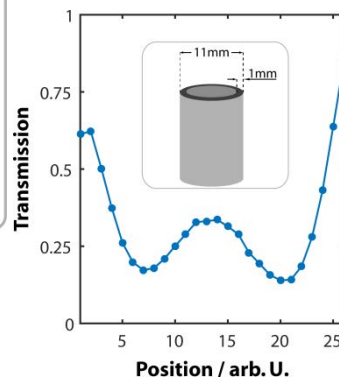


Figure 5. Schematic (inset) and 1D projection of the investigated HDPE cuvette.

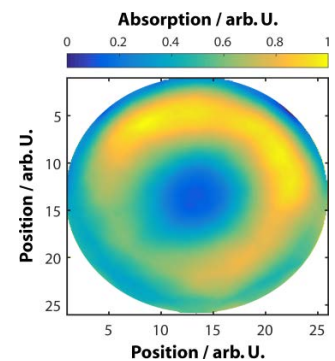


Figure 6. Reconstructed 2D image using all 7 projections.

3.1 Experimental set-up

The experimental set-up is schematically depicted in Fig. 4. An Hg-Arc lamp is installed in a Bruker Vertex 80v Fourier transform spectrometer, which serves as a broadband terahertz source emitting radiation between 0.9 and 3 THz, limited by the beamsplitter and a far-infrared cut-off filter in front of the detecting bolometer. The terahertz radiation is collimated and passes the Michelson interferometer, whereupon the radiation is focused to the sample compartment. Here, it is transmitted through a 1 mm thick HRFZ-Si window and the object under investigation. Finally, a parabolic mirror focuses the radiation onto a liquid He cooled bolometer, which is measuring the total optical intensity. To achieve a spatial modulation of the terahertz radiation, thus yielding the

spatial resolution, the HRFZ-Si window is irradiated by a chopped 808 nm laser diode, which is spatially modulated by a DMD. The photodoping of the Si window leads to a change of its transmission characteristics in the terahertz spectral region, transferring the temporal and spatial modulation of the near infrared radiation to the terahertz radiation.

3.2 Experimental results and discussion

Figure 5 shows the measured spatial transmission through a HDPE cuvette, which serves as sample object. The symmetry of the sample object can be observed clearly. At first, a drop from the high transmissive region of the ambient atmosphere to approximately 0.14 is visible, which represents the outer HDPE wall of the sample. This drop is followed by a rise in transmission to 0.34 through the centre of the object. By recording 7 projections of the object under different rotation angles Ω_z a 2D image is reconstructed. The resulting image is shown in Fig. 6, clearly identifying the physical shape of the HDPE cuvette.

4. CONCLUSIONS

In conclusion, we have studied HSM using only one PCA for two-dimensional spectrally resolved terahertz imaging. The PCA serves simultaneously for the generation and the detection of the CW-terahertz radiation thus simplifying enormously the set-up. The developed frequency-resolved imaging shows promises for security and quality control applications in the near future. This simple and compact terahertz imaging set-up allows a significant cost reduction and relaxes the demand on high power lasers as only one PCA is needed. The applied multiplexing approach in section 3 makes multi-pixel detectors and raster scanning superfluous, allowing the use of superior bucket detectors with high signal to noise ratios. Furthermore, the measurement of interferograms, instead of spectrally integrated intensities, will offer spectrally resolved terahertz tomography.

ACKNOWLEDGEMENTS

We thank TOPTICA Photonics AG for the excellent photomixers, particular A. Deninger for productive discussions and acknowledge the support from “Sensors Towards Terahertz” within the LOEWE platform (1502-2995-11). We acknowledge the support of the COST Action MP1204 “TERA-MIR”. Further we thank G. Birkl, M. Schlosser and F. Stopp for support regarding the ECDLs.

REFERENCES

- [1] J. P. Guillet, B. Recur, L. Frederique, B. Bousquet, L. Canioni, I. Manek-Hönninger, P. Desbarats, and P. Mounaix: Review of terahertz tomography techniques, *J. Infrared Millim. Te.* 35(4), 382-411 (2014).
- [2] P. Dean, Y. L. Lim, A. Valavanis, R. Kliese, M. Nikolić, S. P. Khanna, M. Lachab, D. Indjin, Z. Ikonić, P. Harrison, A. D. Rakić, E. H. Linfield, and A. G. Davies: Terahertz imaging through self-mixing in a quantum cascade laser, *Opt. Lett.* 36, 2587 (2011).
- [3] W. L. Chana, K. Charan, D. Takhar, K. F. Kelly, R. G. Baraniuk, and D. M. Mittleman: A single-pixel terahertz imaging system based on compressed sensing, *Appl. Phys. Lett.* 93, 121105 (2008)
- [4] B. Recur, A. Younus, S. Salort, P. Mounaix, B. Chassagne, P. Desbarats, J-P. Caumes, and E. Abraham: Investigation on reconstruction methods applied to 3D terahertz computed tomography, *Opt. Express* 19(6), 5105-5117 (2011).
- [5] R. Al Hadi, H. Sherry, J. Grzyb, Y. Zhao, W. Forster, H. M. Keller, A. Cathelin, A. Kaiser, and U. R. Pfeiffer: A 1 k-pixel video camera for 0.7 – 1.1 terahertz imaging applications in 65-nm CMOS, *IEEE J. Solid-St. Circuits* 47(12), 2999-3012 (2012).
- [6] J. Zdanevičius, M. Bauer, S. Boppel, V. Palenskis, A. Lisauskas, V. Krozer, and H. G. Roskos: Camera for high-speed THz imaging, *J. Infrared Millim. Te.* 36(10), 986-997 (2015).
- [7] D. Shrekenhamer, C. M. Watts, and W. J. Padilla: Terahertz single pixel imaging with an optically controlled dynamic spatial light modulator, *Opt. Express* 21(10), 12507-12518 (2013).
- [8] R. I. Stantchev, B. Sun, S. M. Hornett, P. A. Hobson, G. M. Gibson, M. J. Padgett, and E. Hendry: Noninvasive, near-field terahertz imaging of hidden objects using a single-pixel detector, *Sci. Adv.* 2(6), e1600190 (2016).
- [9] T. Mohr, S. Breuer, D. Blömer, M. Simonetta, S. Patel, M. Schlosser, A. Deninger, G. Birkl, G. Giuliani, and W. Elsässer: Terahertz homodyne self-mixing transmission spectroscopy, *Appl. Phys. Lett.* 106, 061111 (2015).
- [10] A. Roggenbuck, H. Schmitz, A. Deninger, I. C. Mayorga, J. Hemberger, R. Güsten, and M. Grüninger: Coherent broadband continuous-wave terahertz spectroscopy on solid-state samples, *New J. Phys.* 12, 043017 (2010).
- [11] T. Mohr, S. Breuer, G. Giuliani, and W. Elsässer: Two-dimensional tomographic terahertz imaging by homodyne self-mixing, *Opt. Express* 23(21), 27221-27229 (2015).